IEEE Access
Multidisciplinary | Rapid Review | Open Access Journal

Received April 2, 2021, accepted April 26, 2021, date of publication May 3, 2021, date of current version May 13, 2021.

Digital Object Identifier 10.1109/ACCESS.2021.3077030

An Effective Method for Distinguishing Sleep Apnea and Hypopnea Based on ECG Signals

YAO WANG[1,3], SIYU JI[2], TIANSHUN YANG[2], XIAOHONG WANG[1], HUIQUAN WANG[1,3], XIAOYUN ZHAO[4], AND WANG JINHAI[1]

[1]School of Life Sciences, Tiangong University, Tianjin 300387, China
[2]School of Electronics and Information Engineering, Tiangong University, Tianjin 300387, China
[3]School of Precision Instruments and Optoelectronics Engineering, Tianjin University, Tianjin 300072, China
[4]Respiratory and Critical Care Medicine Department and Sleep Center, Tianjin Chest Hospital, Tianjin 300222, China

Corresponding author: Huiquan Wang (huiquan85@126.com)

This work was supported in part by the National Key Research and Development Program of China under Grant 2019YFC0119400, in part by the National Natural Science Foundation of China under Grant 61701342 and Grant 81901789, in part by the Tianjin Natural Science Foundation under Grant 19JCQNJC13100, in part by the Tianjin Science and Technology Plan Project under Grant 18ZXRHSY00200 and Grant 20ZXGBSY00070, in part by the Science and Technology Development Fund of Tianjin Education Commission for Higher Education under Grant 2018KJ212, and in part by the Science and Technology Plan of Tianjin Jinnan District under Grant 20200116.

ABSTRACT Good sleep quality is essential to our life and work. The two major challenges in evaluating sleep quality are the scoring of sleep stages and sleep apnea detection. In addition to sleep apnea, hypopnea is also a respiratory event that occurs at an equal or even higher frequency compared to that of apnea. However, the two phenomena are not only different in terms of physical manifestation, there are also significant differences in the methods and means of clinical treatment. Therefore, in this study we propose an effective algorithm to distinguish between hypopnea and apnea events. We consider two aspects of feature extraction. On the one hand, from the original time-domain waveform of electrocardiogram signals, we extract the time difference sequence between the appearance of the R-R wave in two adjacent QRS waves (RR intervals) and explore the way they change when apnea and hypopnea event occur. On the other hand, considering that the degree of sequence disorder caused by hypopnea and apnea events is different, multi-scale entropy and complexity are chosen as the features that describe this change. The results obtained using the proposed algorithm show that the classification between hypopnea events and any type of apnea events all reach an accuracy rate greater than 90%. For obstructive apnea events, which occur most frequently among the three different types of apneas, the classification accuracy, sensitivity, specificity and F1-score were 91.78%, 92.21%, 91.30%, 92.20%, respectively. The classification results between central apnea events and hypopnea events reached an accuracy of 93.18%, sensitivity of 95.00%, specificity of 91.67% and F1-score of 92.68%. At the same time, the algorithm achieved an accuracy of 92.59%, sensitivity of 90.38%, specificity of 94.64% and F1-score of 92.16% when classifying mixed apnea and hypopnea events. In the classification of normal breathing, hypopnea events and apnea events, the total accuracy rate achieved was 91.92%, with that for normal breathing reaching 93.62%, for hypopnea events reaching 90.39%, and 91.91% for apnea events, with a Kappa coefficient of 0.99. The algorithm proposed in this study constitutes an efficient and convenient approach for apnea and hypopnea event detection and classification.

INDEX TERMS Sleep apnea, hypopnea, multi-scale entropy, complexity, Heart rate variability analysis.

I. INTRODUCTION

In the short term, lack of sleep can cause mental fatigue and drowsiness during daytime work, while long-term occurrence of the condition can have a significantly negative impact on physical health, such as memory loss, emotional instability, etc. Sleep apnea-hypopnea syndrome (SAHS) events are one of the most common sleep disorders that deteriorate sleep quality, and affect about 5-20% of adults [1], [2]. SAHS will result in recurrent respiratory-related events and both short-term symptomatic consequences and long-term physiologic consequences, which include gasping for air while sleeping, headaches and other adverse outcomes. More importantly, the increased incidence of motor vehicle collisions accidents

The associate editor coordinating the review of this manuscript and approving it for publication was Tu Ngoc Nguyen.

due to driving while drowsy, as well as increased incidence of cardiopulmonary complications, cerebrovascular events and neurocognitive effects are all related to SAHS events.

According to the assessment standards of the American Academy of Sleep Medicine (AASM), hypopnea events are defined as a 30% decrease in oronasal airflow and a 3% decrease in blood oxygen saturation with duration greater than or equal to 10 seconds, while apnea events refer to a reduction in airflow of 90% and up to 100% for a duration of at least 10 seconds [3]. In addition to the differences in physiological characteristics between apnea and hypopnea events, the three types of apnea events, namely obstructive apnea (OA), central apnea (CA) and mixed apnea (MA), are also quite different from each other. Among them, OA events are the most common and serious type of breathing disorders, as they can cause complete obstruction of the upper airway and further relaxation of the throat muscles, thereby hindering breathing during sleep [4]. However, OA only causes the disappearance of the nose and mouth airflow, while chest and abdomen breathing still takes place. CA events occur when the central brain system stops sending signals to the muscles that control breathing, resulting in an interruption of respiratory airflow. However, in this case both nasal oral airflow and chest-abdominal breathing disappear at the same time. MA events manifest as OA events in the first half and CA events in the second half or vice versa.

SAHS events are different from other breathing disorders, as they often occur during night sleep and are more detrimental to cardiopulmonary function [5], [6]. In addition, the total number of apnea events plus hypopnea events that occur during night sleep is an important basis for assessing whether a patient suffers from apnea disease. In other words, the occurrence of apnea or hypopnea events is not necessarily indicative of apnea disease and healthy people will also experience a small number of apnea and hypopnea events. Similarly, according to the evaluation criteria of AASM, healthy people generally have an Apnea-Hypopnea Index (AHI) value of less than 5; a value in the range of 5-15 is indicative of mild apnea disease; 15-30 of moderate apnea disease, while a value greater than 30 is indicative of severe apnea disease. The AHI index is defined as the total number of hypopnea, OA, CA and MA events that occur during a night's sleep process divided by the sleep maintenance time, which is the total time from time at which the person first falls asleep to the last wake-up time during the sleep monitoring process, including intermediate wake periods. Therefore, the detection of apnea and hypopnea events is particularly important. At the same time, early detection of breathing disorders and diagnosis of apnea or hypopnea events can help physicians formulate effective treatment methods for these specific respiratory event types.

The internationally recognized gold standard for evaluating sleep apnea and hypopnea events are based on the evaluation of various physiological signals of the patient's polysomnography (PSG) data throughout the night by professional sleep analysts. These including respiratory airflow, pulse oximetry, chest and abdomen movement, electroencephalograms (EEGs), electromyograms (EMGs) etc. However, on the one hand, PSG equipment is expensive and the number of sensors that required to be worn affects the comfort of night sleep. On the other hand, the requirements for professional sleep analysts are higher. Therefore, the purpose of this study is to propose an efficient, reliable, and easy-to-implement detection and classification algorithm that can be applied to home or clinical wearable applications to assist diagnosis of hypopnea and apnea events to solve the problem that due to external factors, PSG data cannot be recorded in time for apnea and hypopnea event assessment.

ECG signals were one of the earliest bioelectric signals studied and applied in the medical field. There have been many related studies on the use of ECG signals in the medical field, especially respiratory related diseases. ECG has a strong periodicity and is more stable during night sleep, as it is not easily disturbed by other bioelectric signals or interference noise. The Heart Rate Variability (HRV) metric, which is extracted from ECG signals, contains three different frequency bands namely Very-Low Frequency (VLF), Low Frequency (LF) and High Frequency (HF), where the power or amplitude of each frequency band is representative of different information and activities of the nervous system.

As mentioned earlier, the pathogenesis of CA events is directly related to the brainstem's respiratory center dysfunction and usually caused by damage to the cerebral hemispheres or various centers in the brainstem. Although the pathogenesis of OA events is not directly related to the brainstem respiratory center, it will cause a gradual decrease in blood oxygen, a gradual increase of negative pressure in the pharynx cavity and a gradual increase in the partial CO_2 pressure during the occurrence of OA events. These phenomena all stimulate the corresponding chemical and baroreceptors to activate the brainstem reticulum system, thus causing short-term awakening. MA events are composed of OA and CA events that alternate, therefore their pathogenesis is also related to brainstem nerves. However the pathogenesis of hypopnea events is different from that of apnea events, as it is caused by reduced alveolar ventilation in both lungs. That is to say, hypopnea events have nothing to do with brainstem nerves. Therefore, brainstem nerve activity will have different manifestations when different breathing events occur. ECG signals have better stability during night sleep and their related characteristics can reflect detailed activities and information of the brainstem nerve system. They are also easy to obtain from flexible wearable devices, whether for home applications or clinical auxiliary diagnosis. Therefore, in this study ECG signals are the research object for the detection and classification of hypopnea and apnea events.

In this study, three issues were taken into consideration for the development of the proposed algorithm. The first issue is the detection of SAHS events; the second is the classification of hypopnea events and any type of apnea events; the third is the distinction between normal breathing, hypopnea events and apnea events. That is to say, the purpose of this

article is to propose an algorithm that can solve the above three problems simultaneously. In addition, the characteristics of ECG signals considered from the following two main aspects. The first is to extract relevant HRV indicators from the RR interval sequence obtained from the original time-domain waveform, while the second is to extract the nonlinear dynamic characteristic index from the frequency band with the main energy concentration corresponding to the original sequence. Finally, the features obtained by the two main aspects are combined for feature screening, so that features with low contribution rates can be eliminated, and remaining features input in machine learning classification models to obtain feature evaluation indicators.

The results obtained by the proposed algorithm in this study show that it can solve the above problems simultaneously, reaching an accuracy of 97.96%, sensitivity of 98.10%, specificity of 97.83% and F1-score reached 98.10% in the detection of apnea and hypopnea events. At the same time, the classification between hypopnea events and any type of apnea events reached more than 90% accuracy. The detailed results are as follows: The classification results of OA and hypopnea events respectively have an accuracy of 91.78%, sensitivity of 92.21%, specificity of 91.30% and F1-score of 92.20%. The classification accuracy, sensitivity, specificity and F1-score of CA and hypopnea events were 93.18%, 95.00%, 91.67%, and 92.68%, respectively. An accuracy of 92.59%, sensitivity of 90.38%, specificity of 94.64%, and F1-score of 92.16% were obtained when MA and hypopnea events were classified. In addition, in the classification of normal breathing, hypopnea events, and apnea events, the total accuracy obtained reached 91.92%. Among them, the classification accuracy of normal breathing, hypopnea events and apnea events were 93.62%, 90.39% and 91.91% respectively, with a kappa coefficient of 0.99. The results show that the algorithm can be used in clinical or home diagnosis of apnea and hypopnea events and has certain clinical significance.

II. RELATED WORK

Many researchers have applied other physiological signals such as oxygen saturation (SaO_2), EEG, Respiratory signal etc. for the detection of sleep apnea and hypopnea events. In sleep medicine, nocturnal pulse oximetry provides a useful tool for the analysis of respiratory patterns and has been successfully applied in the field of detecting SAHS events. Non-linear features from nocturnal SaO_2 recordings were used to discriminate between obstructive sleep apnea syndrome positive and negative patients, Approximate Entropy, Central Tendency Measure and Lempel-Ziv complexity were extracted as features, and the selected MLP (multilayer perceptron)-based classifier provided a diagnostic accuracy of 85.5% (89.8% sensitivity and 79.4% specificity) [13]. A feature-extraction stage based on nocturnal pulse oximetry was also implemented, where 16 features (time and frequency statistics, as well as spectral and non-linear features) were computed, and a genetic algorithm approach was applied in the feature selection stage. The methodology achieved 87.5% accuracy (90.6% sensitivity and 81.3% specificity) in the test set using a logistic regression classifier [14].

Instead of utilizing several physiological signals, the EEG signal alone is receiving special attention by the researches because of its successful application in analyzing sleep-related problems; it has also been applied to the detection of sleep apnea events. For example, an automatic apnea detection scheme has been proposed using a single-lead EEG signal to discriminate apnea patients and healthy subjects, as well as to deal with the difficult task of classifying apnea and non-apnea events of an apnea patient. For this purpose, a unique multi-band sub-frame-based feature extraction scheme was developed to capture the feature variation pattern within a frame of EEG data, and the accuracy, specificity and sensitivity reached 90.60%, 84.11% and 97.10% respectively [15]. A new technique for recognizing patients with OSAS was also introduced using bi-spectral characteristics of EEG signal and an artificial neural network (ANN). The amount of quadratic phase-coupling in each sub-band of EEG (namely: delta, theta, alpha, beta and gamma) was calculated over the bi-spectral density of the EEG, and the system achieved an accuracy of 96.15% [16].

Respiratory signals provide a convenient and less invasive choice to develop automated SAHS event detection algorithms compared to other PSG signals. Besides, the AASM also defines SAHS events on the basis of the amplitude oscillation in flow and pressure signals, respectively. Respiratory signals have been applied for classifying SAHS events since the field's early years. Examples methods include combining the discrete wavelet transform (DWT) and ANNs, where the abdominal and thoracic respiration signals were separated into spectral components by using multi-resolution DWT, and the energy of these spectral components was applied as an input to an ANN, achieving accuracies of 73.42%, 94.23% and 66.16% for OA, CA, MA [17]. More recently, a new algorithm was developed by Kim, J, *et al.* to derive a respiratory baseline from the oronasal airflow signal in order to detect sleep apnea events using a dynamically adjusted threshold classification approach. This new algorithm achieved a sensitivity of 80.0%, specificity of 88.7%, and an area under receiver operating characteristics curve (AUC) of 0.844 [28]. The results show that this new algorithm can potentially generalize over patients with different apnea severity levels and longer monitoring periods effectively. A new probabilistic algorithm for automated detection of apnea events during sleep based only on the oronasal respiration signal was also proposed last year. The proposed model leverages the AASM's recommendations for characterizing apnea events with respect to dynamic changes in the local respiratory airflow baseline, which is different from classical threshold-based classification models. However, a Gaussian mixture probability model for detecting sleep apnea based on the posterior probabilities of the respective events was used [29]. The results obtained by this new algorithm were TPR = 88.5%, TNR = 82.5%, and AUC = 86.7%, which shows a significant improvement in the

ability to detect sleep apnea events compared to rule-based classifiers.

In the present study, ECG signals are used as the research object, and the detection and classification of SAHS events are carried out by combining the related characteristics of HRV and nonlinear dynamics. At the same time, OA, CA and MA events are all considered. The proposed algorithm in our study not only achieves an accuracy of 97.96%, sensitivity of 98.10%, specificity of 97.83% and F1-score of 98.10% in detecting SAHS events, but also achieves classification accuracies of 90% and above for distinctions between hypopnea events and the three different types of apnea events.

III. MATERIALS AND METHODS

A. SLEEP APNEA AND HYPOPNEA DATASET

To verify the proposed algorithm, PSG data from 25 Tianjin Chest Hospital clinical apnea patients with large differences in AHI values were used as the research object. The AHI refers to the number of occurrences of SAHS events per hour during night sleep and it is the basis for measuring the severity of patient apnea. The ECG signal obtained from the ECG-I and ECG-II channels at a sampling frequency of 200 samples per second was adopt. We enlisted professional sleep analysts also from Tianjin Chest Hospital to mark apnea and hypopnea events according to the evaluation standards of the AASM, to obtain ground truth labels. Among the 25 apnea patients, 14 people were considered severe, as they had an AHI > 30; 7 people were considered moderate, with AHI values between 15 and 30; mild patients were 4 people with AHI values between 5 and 15. Except for patients with apnea, the ECG data of 3 normal people were used to construct a data set of normal sleep states, for which AHI < 5. The Body Mass Index (BMI) values were 18, 27, and 22 respectively. The detailed information of the study group is shown in Table 1 and the sample size for each event is shown in Table 2.

The PSG data used in this study were previously archived anonymized data with the patient's personal biological information erased so as to preserve the confidentiality of the patients' identities. The study was reviewed by the ethics committee of the authors' unit and was found to meet the requirements of ethics exemption, so the patients' whose data were used did not need to sign an informed consent form.

TABLE 1. Detailed information of apnea patients. (Duration is 10 seconds).

Patient ID	Gender	Age	AHI	BMI
SG001	M	61	56.9	34
SG002	M	51	37.7	26
SG003	M	52	46.3	20
SG004	F	71	20.5	31
SG005	M	50	43.9	24
SG006	M	41	22.0	25
SG007	M	53	49.0	23
SG008	M	64	54.5	29
SG009	M	58	16.7	25
SG010	F	58	46.4	31
SG011	M	66	24.2	28
SG012	M	76	5.7	24
SG013	M	71	13.9	29
SG014	F	62	52.5	32
SG015	M	61	38.0	29
SG016	F	69	25.7	22
SG017	M	65	6.0	25
SG018	M	56	46.9	26
SG019	M	76	11.3	34
SG020	F	62	34.9	27
SG021	M	59	48.1	29
SG022	M	77	19.1	27
SG023	M	59	16.5	23
SG024	F	39	53.4	39
SG025	M	61	84.2	40

TABLE 2. Number of samples for each respiratory and normal event (duration is 10 seconds).

Type of samples	Number of samples
Hypopnea	550
Obstructive apnea	400
Central apnea	247
Mixed apnea	308
Normal	550

B. FEATURE EXTRACTION – HEART RATE VARIABILITY

HRV is a characteristic index that reflects small changes and differences in the RR interval sequence of ECG signals. The mechanism is that the sympathetic nerve and the vagal nerve coordinate to control the pacing of the sinus node, and specific performance is irregular changes in the length of each cardiac cycle. Changes in the time-domain waveform of the ECG signal during SAHS events are observable. The detailed changes are shown in Figure 1. As mentioned earlier, the pathogenesis of OA and CA events are both related to the nervous system in different ways. The HRV frequency domain measurements can reflect very small change in autonomic nervous systems and overall activity of the sympathetic. Therefore, the characteristics of the RR interval extracted from the time domain were selected to show the characteristics of different types of respiratory events. The specific features extracted are shown in Table 3.

The interpretation of the time domain features is as follows: The mean and standard deviation reflect the degree of dispersion of the RR interval series and measure the uncertainty of the sequence; RMSSD is the root mean square of the difference between adjacent RR intervals, which expresses the degree of fluctuation of the time interval between adjacent RR intervals; SDSD is the difference between the maximum and minimum of the RR interval series. The meaning of

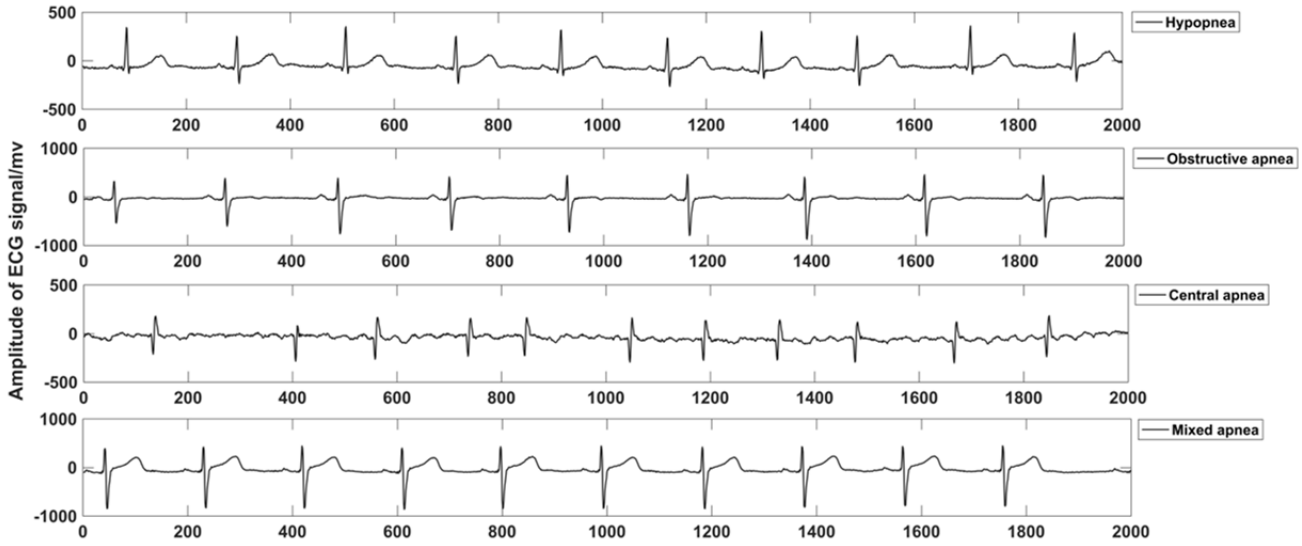

FIGURE 1. 10-second comparison chart of ECG time-domain waveforms between hypopnea, OA, CA, and MA events.

TABLE 3. Characteristic detailed information (RR interval with outliers removed).

Physiological signal	Time domain characteristics	Frequency domain characteristics
ECG-I + ECG-II	MEAN STD RMSSD SDSD	VLF Total Power LFn LFn/HFn

frequency domain features is as follows: VLF corresponds to the frequency band power between 0.003Hz-0.04Hz, reflecting the auxiliary information of sympathetic nerves; Total Power is between 0.003Hz-0.4Hz frequency band power, reflecting dominant sympathetic nerve activity and overall activity of the autonomic nervous system; LFn/HFn is the ratio of the normalized low frequency power (LFn) to the normalized high frequency power (HFn), which is a characteristic that reflects the overall balance between the sympathetic nerves and the parasympathetic nerves. The frequency range of LFn is 0.04Hz-0.15Hz, while that of HFn is 0.15Hz-0.4Hz.

C. FEATURE EXTRACTION – LEMPEL-ZIV COMPLEXITY

Lempel-Ziv complexity analysis is based on a coarse-grained of the measurements [18]. It is a way to characterize the rate at which new patterns appear in a time series. First, an ECG signal preprocessing step is applied by removing the direct current (DC) component and normalizing, which eliminates the influence of external interference on the original ECG data. Since other frequency components are significant, the DC offset of an ECG frame is eliminated first by subtracting the mean value of that frame from each sample value. After removing the DC component, amplitude normalization is necessary to eliminate undesirable fluctuations in the same category. After that, a fast Fourier transform is applied on the preprocessed data to obtain the main energy concentration band. The transform output is filtered using an infinite impulse response Butterworth filter to obtain the data corresponding to this frequency band, which best reflect the degree of sequence change.

In order to perform a detailed analysis of the sequence, we did not directly analyze the complexity of the data in the main energy concentration bands but expanded discrete wavelet transform (DWT). Lempel-Ziv analysis was applied to the high frequency coefficients obtained from the DWT. The detailed algorithm for obtaining the Lempel-Ziv complexity is as follows:

1. Perform sequence binarization for the 10s-long ECG data segment (S) whose complexity is to be determined. Taking $a = median(S)$ as a threshold, set the values for which $S(k) \geq a$ as equal to 1, and 0 otherwise, where $k = 1, 2, 3, \ldots, length(S)$.
2. Initially set the number of new modes to 1 and use $c(n)$ to indicate, that is $c(n) = 1$.
3. Construct $S = S(1)$ as the initial sequence S, $Q = S(2)$ as the initial Q sequence, and define the SQ sequence as the concatenation of the S and Q sequences, namely $SQ = [S, Q]$, The SQv sequence is the binary sequence obtained by subtracting the last data point from the SQ sequence.
4. At this time, determine whether Q is a substring (subsequence) of SQv; if it is, then Q is a sequence that can be copied from S rather than a new sequence, and S does not need to be changed. The Q sequence is updated to $[S(2), S(3)]$ and it is judged again whether Q is a subset of the SQv sequence (the SQv sequence has been

updated at this time). In the same manner, update Q sequentially to judge.

5. Repeat step 3 until Q does not belong to the SQv sequence. At this point, Q is no longer a subsequence of SQv but a new sequence. Then, the number of new modes increases by 1, that is $c(n) = c(n)+ 1$. S is also updated $S = [S, Q]$ at this time. $S = [\, S(1), S(2), S(3), S(4), S(5), \ldots, S(r), S(r+ 1), \ldots, S(r + k)\,]$, where r is the current data index value. Q is updated to $Q = [S(r + k+ 1)\,]$. Repeat step 3.
6. The calculation is stopped when Q reaches the last element of the sequence, and the value of $c(n)$, the number of different subsequences, is obtained.
7. In order to obtain the complexity measure of independence, the normalized $c(n)$ is used in this study: Suppose the number of different symbols in a symbol set A is α and the length of the sequence $P \in A^*$ is $l(p) = n$, where A^* denotes the set of all finite-length sequences over the finite symbol set A. The upper bound of $c(n)$ is given by

$$c\,(n) < \frac{n}{(1 - \varepsilon_n) * log(n)} \tag{1}$$

where ε_n is a small quantity and $\varepsilon_n \to 0$ $(n \to \infty)$. Therefore, in general, $n/\log(n)$ is the upper bound of $c(n)$, where $n = l(p)$ and the base of log is α, *i.e.*,

$$\lim_{n\to\infty} c\,(n) = b\,(n) \equiv \frac{n}{log_\alpha(n)} \tag{2}$$

For a *0-1* sequence, $\alpha = 2$, therefore

$$b(n) \equiv \frac{n}{log_2(n)} \tag{3}$$

$C(n)$ can be normalized via this limit

$$C\,(n) = \frac{c\,(n)}{b\,(n)} \tag{4}$$

D. FEATURE EXTRACTION – MULTI-SCALE ENTROPY

Entropy is an effective method to measure the complexity of time series. Approximate entropy (ApEn) was developed by Pincus as a measure of regularity to quantify the levels of complexity within a time series, and was an improved approach based on entropy [19]. Richman *et al.* ameliorated the ApEn algorithm and obtained the sample entropy (SpEn) [20]. ApEn and SpEn have been widely used for the analysis of physiological signals [21]–[24]. In this study, the SpEn of the sequence at multiple scales was selected as a feature to measure the complexity of the ECG sequence. It was proposed by Costa *et al.* and named multi-scale entropy (MSE).

We apply the same signal preprocessing steps as the Lempel-Ziv complexity analysis and obtain the corresponding multi-scale entropy of the wavelet coefficients. The calculation process of multi-scale entropy is as follows:

1. First, a discrete sequence of length N is formed, $x = \{x(1), x(2), x(3), \ldots, x(n)\}$, according to the equation:

$$y_j^{(\tau)} = \frac{1}{\tau} \sum\nolimits_{i=(j-1)\tau+1}^{j\tau} x_i, \quad 1 \le j \le \frac{N}{\tau} \tag{5}$$

In this manner, we construct continuous coarse-grained time series on multiple scales, where τ is the scale factor. The length of each coarse-grained time series is equal to the length of the original time series divided by the scale factor. In the coarse-grained time series corresponding to each scale, we use m as the dimension of the sequence formed to find the sample entropy.

2. Follow the process below to calculate sample entropy under different scale factors separately:
   (1) First, form the input as the m-dimensional data sequence $X_m(i) = \{y_{i+k}, 0 \le k \le m - 1\}$
   (2) For each i, calculate the distance between $X_m(i)$ and the remaining vector $X_m(j)$:

$$\begin{aligned} d\,[X_m\,(i)\,, X_m\,(j)] = max|y_{(i+k)} - y_{(j+k)}|, \\ (0 \le k \le m - 1, \\ i, j{=}1 \sim M - m + 1, i{\neq}j) \end{aligned} \tag{6}$$

   (3) Set the tolerance threshold during the matching process as $r > 0$, then count the number of $d\,[X_m\,(i)\,, X_m\,(j)] < r, (i, j = 1 \sim M - m + 1, i \neq j)$ for each i. Set $B^m(i)$ as the number of template matches and calculate the ratio of $B^m(i)$ to the total distance, denoted as:

$$C_\tau^m(r) = \frac{B^m(i)}{M - m} \tag{7}$$

   (4) Calculate the average of $C_\tau^m(r)$:

$$C^m(r) = (M - m + 1)^{-1} \cdot \sum\nolimits_{i=1}^{M-m+1} C_\tau^m(r) \tag{8}$$

   (5) Increase the dimension to $m+ 1$ and repeat the above. Calculate $C_\tau^{m+1}(r)$ according to the following equation:

$$C_\tau^{m+1}\,(r) = \frac{B^{m+1}\,(i)}{M - m + 1} \tag{9}$$

   (6) Calculate the average of $C_\tau^{m+1}(r)$:

$$C^{m+1}(r) = (M - m)^{-1} \cdot \sum_{i=1}^{M-m} C_\tau^{m+1}\,(r) \tag{10}$$

   where M is a finite value. Based on the above steps, the estimated sample entropy value when the sequence length is M is:

$$SampEn(m, r, M) = -log[\frac{C^{m+1}\,(r)}{C^m\,(r)}] \tag{11}$$

   (7) Repeat the above process to obtain the sample entropy values at different scales.

E. FEATURE SELECTION – RELIEFF ALGORITHM

The Relieff feature selection method is an improved version of the Relief feature weighting algorithm. The main limitations of the Relief algorithm are that it cannot handle incomplete data and can only handle two categories of data. The Relieff algorithm, proposed by Kononenko *et al.* [27], improves the limitations of the Relief algorithm. In this study, the Relieff feature screening method was adopted. The detailed steps of the Relieff algorithm are as follows:

(1) Denote the input feature set as D, the sample sampling time as m and the number of nearest neighbor samples as k. The output is the feature statistics index T of each feature.
(2) Set all statistics indicators to 0;
(3) E is a sample data randomly extracted from the feature set D. The k nearest neighbors of the same category of E in the total sample set are marked as:

$$H_j \quad (j = 1, 2, \ldots k) \tag{12}$$

Find the k nearest neighbors from the feature set that are inconsistent in each category and mark them as:

$$M_j\,(C) \quad (j = 1, 2, \ldots k) \tag{13}$$

(4) Calculate the statistical indicators for each feature A as follows. $p(C)$ is the proportion of a category, $p(Class(E))$ is the proportion of the class of a sample randomly selected

$$\begin{aligned} W(A) = W(A) &- \sum\nolimits_{j-1}^{k} diff\,(A, E, H_j)/(m \cdot k) \\ &+ \sum\nolimits_{C \notin class(R)} \left[\frac{p\,(C)}{1 - p\,(Class\,(E))}\right. \\ &\times \left.\sum\nolimits_{j-1}^{k} diff\,(A, E, H_j)\right]/(m \cdot k) \end{aligned} \tag{14}$$

$$diff\ (A, E_1, E_2) = \begin{cases} 0 \\ \dfrac{|E_1\,[A] - E_2\,[A]|}{max(A) - min(A)} \\ 1 \end{cases} \tag{15}$$

If A is discrete and $E_1[A] = E_2[A]$, the value of *diff* is 0; If A is discrete and $E_1[A] \neq E_2[A]$, the value of *diff* is 1; if A is continuous, the value of *diff* is $\dfrac{|E_1[A] - E_2[A]|}{max(A) - min(A)}$

(5) Repeat the above steps m times and update the statistical indicators of each feature;
(6) Finally, after sorting from largest to smallest according to statistical indicators' values, select the top-ranked features to get a suitable feature set.

We then combine the above feature extraction and feature screening methods to process the ECG signals. The final result of feature screening is used as the input to the classifier. The characteristics are evaluated from the following three aspects. The first aspect is the performance of the proposed algorithm in detecting SAHS events. The second is the algoritghm's classification accuracy between hypopnea events and the three types of apnea events. The third is the ability of the proposed algorithm distinguish between the three categories of normal breathing, hypopnea events and apnea events. The detailed feature extraction and screening flowchart is shown in Figure 2.

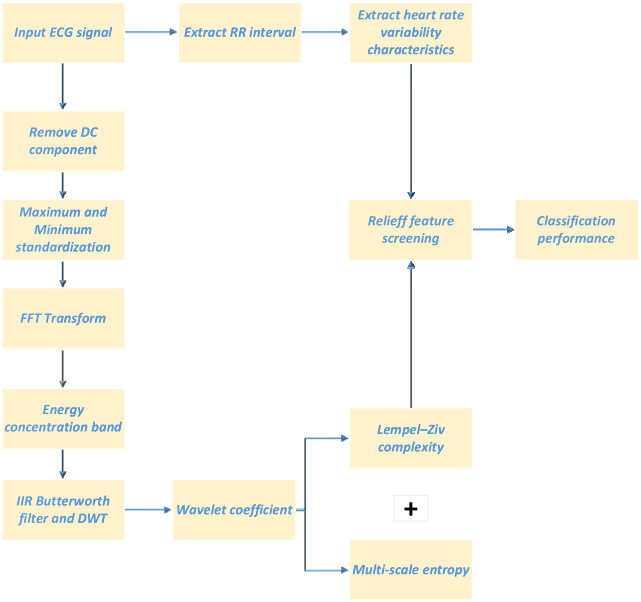

FIGURE 2. Detailed steps of feature extraction and screening.

IV. RESULTS

A. DECISION TREE CLASSIFIER

The flexibility of the decision tree classifier not only can finish well for improving the classifier performance in general which can maximize accuracy and minimize computational requirements, but also can treating special applications [25]. The random forest classifier, proposed by Breiman, is one of the representatives of decision tree classifiers, and consists of a combination of tree classifiers, where each classifier is generated using a random vector sampled independently from the input vector and each tree casts a unit vote for the most popular class to classify an input vector [26]. This classification algorithm can handle a large number of input variables and can generate an unbiased estimate of the generalized error internally. Its simultaneous processing capability makes it efficient and less time-consuming. In this study, in addition to the random forest (RF) algorithm, the ensemble (Ens) method of comprehensive judgment based on the prediction results of multiple decision trees is also considered to determine the final result of the classifier. The detailed schematic diagram of the RF algorithm is shown in Figure 3; the classification principle of the Ens learning classifier is similar to that of the RF. In addition to decision tree classifiers, non-decision tree classifiers, such as the support vector machine (SVM) and k-nearest neighbor (KNN) classifiers, are also implemented to evaluate the effectiveness of the proposed algorithm.

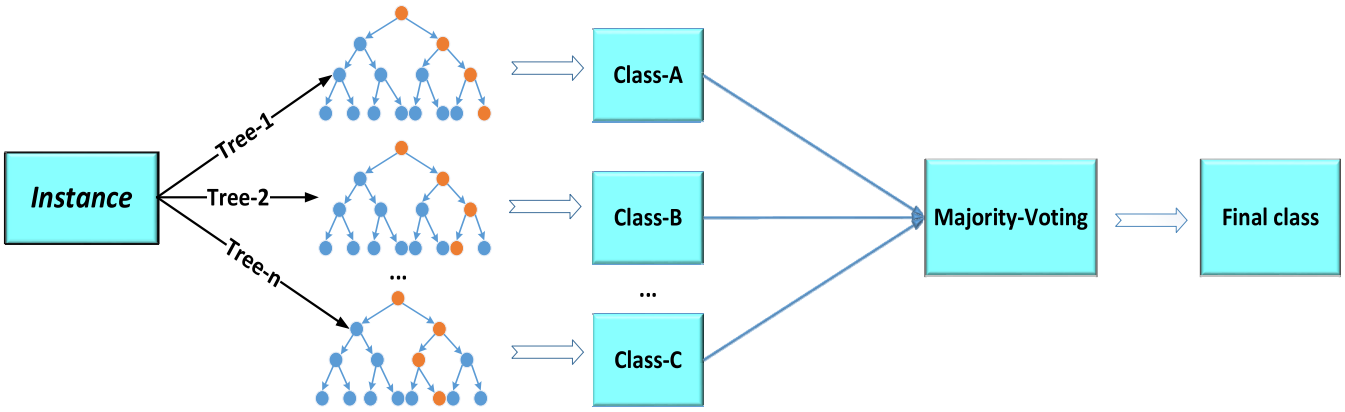

FIGURE 3. Random forest classifier.

B. EVALUATION INDICES

In order to verify the effectiveness of the model more comprehensively, for the two-class model, besides accuracy, indicators such as sensitivity, specificity, and *F1-score*, calculated using the *TP*, *TN*, *FP*, and *FN* parameters are introduced. The calculation equations are:

$$accuracy = \frac{TP + TN}{TP + TN + FP + FN} \tag{16}$$

$$Sensitivity = \frac{TP}{TP + FN} \tag{17}$$

$$Specificity = \frac{TN}{TN + FP} \tag{18}$$

$$F1 - Score = 2 * \frac{Precision * Recall}{(Recall + \Pr ecision)} \tag{19}$$

where *TP* is the number of samples where a positive class sample is predicted as such; *TN* is the number of samples that are correctly identified as belonging to the negative class; *FP* is the number of negative class samples predicted as positive; and *FN* is the number of positive class samples predicted as negative.

For three different types of samples classification, the model evaluation index is different from the two-class model. In addition to the accuracy of each type of sample, the kappa coefficient obtained using the confusion matrix is selected as an evaluation index of the three-class model. The calculation equation is:

$$k = \frac{p_o - p_e}{1 - p_e} \tag{20}$$

where p_o is the sum of the number of samples correctly classified in each category divided by the total number of samples, i.e. the overall classification accuracy. The total number of samples is n; if the number of true samples in each category respectively is $\alpha_1, \alpha_2, \alpha_3 \ldots \alpha_c$, and the number of samples obtained by the prediction in each category is respectively is $b_1, b_2, b_3, \ldots, b_c$, then the calculation equation of p_e is as follows:

$$p_e = \frac{a_1 \times b_1 + a_2 \times b_2 + \ldots + a_c \times b_c}{n \times n} \tag{21}$$

C. RESULTS OF DETECTING SLEEP APNEA HYPOPNEA EVENTS

Based on the number of samples obtained in Table 2 and considering sample balance, 550 samples were selected from the normal breathing and the SAHS events' sample sets. Apnea and hypopnea events were divided on a 1:1 ratio and the set of apnea events was divided again on a ratio of OA: MA: CA = 6:3:1, which is considered by professional respiratory disease experts as a reasonable ratio based on years of clinical experience. In order to ensure the reliability of the evaluation results, 10% of the total data set was randomly selected for Relieff feature screening. Based on the results of feature screening, the remaining 90% of the samples are randomly divided into training, validation, and test sets on a 6:2:2 ratio, and the results of the test set were used for final model classification results. The results of feature screening were as follows:

(1) The mean value of RR intervals based on ECG-I and ECG-II;
(2) The standard deviation (STD) of the multi-scale entropy (MSE) of the second layer of the high-frequency coefficients (HFCs) corresponding to the DWT of the signal in the main concentrated frequency band (CFB) of the ECG-I energy;
(3) The mean of MSE of the third and second layers of HFC corresponding to DWT of the signal in the main CFB of ECG-II energy;
(4) The STD of the MSE of the third layer of the HFC corresponding to the DWT of the signal in the main CFB of ECG-II energy;
(5) VLF and SDSD of the RR interval of ECG-II;
(6) The mean of MSE of the third and second layers of the HFCs corresponding to DWT of the signal in the main CFB of ECG-I energy;
(7) The Lempel–Ziv complexity of the fourth layer of the HFCs corresponding to DWT of the signal in the main CFB of ECG-II energy;

The above 11 features are considered to be the optimal feature set. The detailed classification results are shown

TABLE 4. Classification results of normal breathing and SAHS events.

Classifier	Accuracy	Sensitivity	Specificity	F1-score
RF	95.94%	96.63%	95.37%	95.56%
Ens	97.96%	98.10%	97.83%	98.10%
SVM	91.88%	95.83%	88.12%	92.00%
KNN	88.33%	87.96%	88.76%	89.20%
Mean	93.53%	94.63%	92.52%	93.72%
Std	4.28%	4.54%	4.82%	3.91%

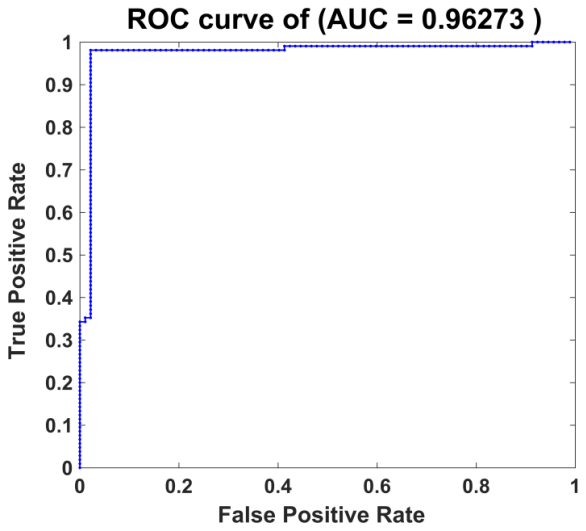

FIGURE 4. The ROC curve and AUC value corresponding to the classification result of detecting respiratory events.

in Table 4, where normal is defined as negative and SAHS events are defined as positive. The ROC curve is shown in Figure 4.

D. RESULTS OF CLASSIFICATION BETWEEN HYPOPNEA AND OBSTRUCTIVE APNEA EVENTS

In this part, 400 samples were selected from the hypopnea and the OA events sample sets. Similarly, 10% of the total data set were extracted for Relieff feature screening. Based on the results of feature screening, the remaining 90% of the samples were randomly divided into training, validation and test sets on a ratio of 6:2:2, and the results of the test set were used to obtain the final model classification results. The results of feature screening were as follows:

TABLE 5. Classification results of hypopnea events and OA events.

Classifier	Accuracy	Sensitivity	Specificity	F1-score
RF	91.78%	92.21%	91.30%	92.20%
Ens	91.55%	90.79%	92.42%	92.00%
SVM	87.32%	87.18%	87.50%	88.31%
KNN	86.21%	92.31%	81.25%	85.71%
Mean	89.21%	90.62%	88.12%	89.56%
Std	2.86%	2.39%	5.04%	3.12%

(1) The mean value of the RR interval of ECG-I and ECG-II;
(2) RMSSD and SDSD of the RR interval of ECG-I;
(3) RMSSD of the RR interval of ECG-II;
(4) Total power of the RR interval of ECG-I;
(5) LFn of the RR interval of ECG-I and ECG-II;
(6) LFn/HFn of the RR interval of ECG-I and ECG-II;
(7) The mean of MSE of the second and third layer of the HFCs corresponding to the DWT of the signal in the main CFB of ECG-I and ECG-II energies;
(8) The STD of the MSE of the second and third layer of the HFCs corresponding to DWT of the signal in the main CFB of ECG-I and ECG-II energies;
(9) The Lempel-Ziv complexity of the third and fourth layer of the HFCs corresponding to the DWT of the signal in the main CFBs of the ECG-I and ECG-II energy;

The above 22 features were considered to be the optimal feature set. The detailed classification results are shown in Table 5, where hypopnea events are defined as negative and OA events as positive. The ROC curve is shown in Figure 5.

E. RESULTS OF CLASSIFICATION BETWEEN HYPOPNEA AND CENTRAL APNEA EVENTS

In this part, 247 samples were selected from the hypopnea and the CA event sample sets. 10% of the total data set were extracted for Relieff feature screening. Based on the results of feature screening, the remaining 90% of the samples were randomly divided into training, validation and test sets on a ratio of 6:2:2. The results of the test set were used to obtain the final model classification results. The results of feature screening are as follows:

(1) LFn and LFn/HFn of the RR interval of ECG-I and ECG-II;

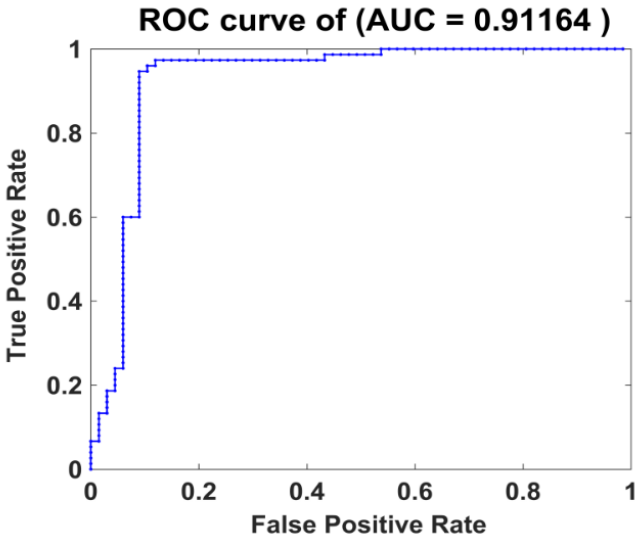

FIGURE 5. The ROC curve and AUC value corresponding to the classification result of hypopnea and OA events.

(2) The STD and mean of the MSE of the second layer of HFCs corresponding to DWT of the signal in the main CFB of ECG-I energy;
(3) The Lempel-Ziv complexity of the second and fourth layers of the HFCs corresponding to the DWT of the signal in the main CFB of ECG-II energy;
(4) The mean value of the RR interval of ECG-I and ECG-II;
(5) The mean of the MSE of the second layer of the HFCs corresponding to the DWT of the signal in the main CFB of ECG-II energy;
(6) The STD of the RR interval of ECG-II;
(7) The Lempel-Ziv complexity of the third and fourth layers of the HFCs corresponding to the DWT of the signal in the main CFB of ECG-I energy;
(8) The SDSD of the RR interval of ECG-II;
(9) The STD of MSE of the second layer of the HFCs corresponding to the DWT of the signal in the main CFB of ECG-II energy;
(10) The STD and mean of MSE of the third layer of the HFCs corresponding to the DWT of the signal in the main CFB of ECG-I energy;

The above 18 features were considered to be the optimal feature set. The detailed classification results are shown in Table 6, where hypopnea events are defined as negative and CA events are positive. The ROC curve is shown in Figure 6.

F. RESULTS OF CLASSIFICATION BETWEEN HYPOPNEA AND MIXED APNEA EVENTS

In this part, 308 samples were selected from the hypopnea and MA event sample sets. As per the other cases, 10% of the total data set were used for Relieff feature screening. Based on the results of feature screening, the remaining 90% of the samples were randomly divided into training, validation and test sets on a 6:2:2 ratio. The results of the test set were used

TABLE 6. Classification results of hypopnea and CA events.

Classifier	Accuracy	Sensitivity	Specificity	F1-score
RF	93.18%	95.00%	91.67%	92.68%
Ens	92.05%	91.67%	92.50%	92.63%
SVM	88.63%	91.84%	84.62%	90.00%
KNN	89.77%	93.18%	86.36%	90.11%
Mean	90.91%	92.92%	88.79%	91.36%
Std	2.08%	1.54%	3.88%	1.50%

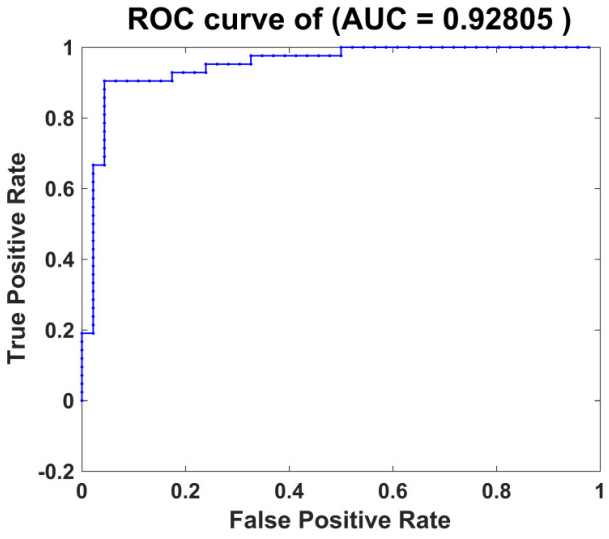

FIGURE 6. The ROC curve and AUC value corresponding to the classification result of hypopnea and CA events.

to obtain the final model classification results. The results of feature screening are as follows:

(1) The STD and mean of the RR interval of ECGI and ECG-II;
(2) RMSSD and SDSD of the RR interval of ECGI and ECG-II;
(3) VLF and total power of the RR interval of ECG-II;
(4) LFn and total power of the RR interval of ECG-I;
(5) LFn / HFn of the RR interval of ECG-I and ECG-II;
(6) The mean of MSE of the third layer of the HFCs corresponding to the DWT of the signal in the main CFB of ECG-I and ECG-II energies;

TABLE 7. Classification results of hypopnea and MA events.

Classifier	Accuracy	Sensitivity	Specificity	F1-score
RF	91.67%	92.31%	91.07%	91.43%
Ens	92.59%	90.38%	94.64%	92.16%
SVM	89.81%	96.15%	83.93%	90.09%
KNN	88.89%	92.30%	85.71%	88.88%
Mean	90.74%	92.79%	88.84%	90.64%
Std	1.69%	2.41%	4.91%	1.45%

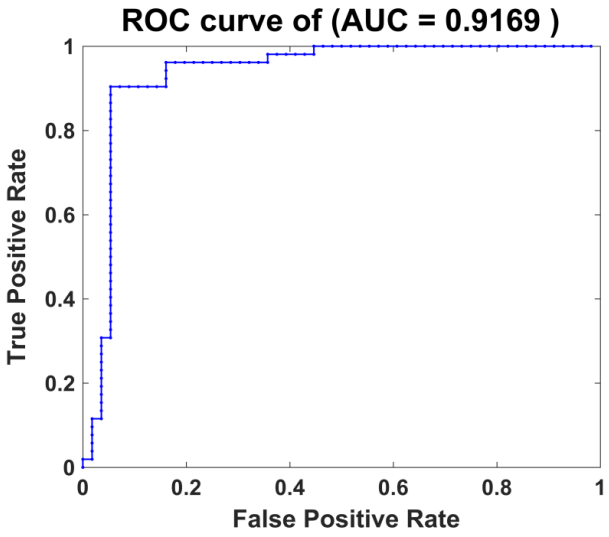

FIGURE 7. The ROC curve and AUC value corresponding to the classification result of hypopnea and MA events.

(7) The STD of MSE of the second and third layers of the HFCs corresponding to the DWT of the signal in the main CFB of ECG-II energy;
(8) The STD of MSE of the second layer of the HFCs corresponding to the DWT of the signal in the main CFB of ECG-I energy;
(9) The Lempel-Ziv complexity of the second layer of the HFCs corresponding to DWT of the signal in the main CFB of ECG-I energy;

The above 20 features were considered to be the optimal feature set. The detailed classification results are shown in Table 7, where hypopnea events are defined as negative and MA events as positive. The ROC curve is shown in Figure 7.

TABLE 8. Classification results of normal breathing, hypopnea events and apnea events.

Classifier	Normal	Hypopnea	Apnea	Kappa
RF	93.62%	90.39%	91.91%	0.99
Ens	92.66%	90.12%	91.59%	0.99
SVM	92.71%	76.52%	91.86%	0.99
KNN	91.18%	79.17%	92.93%	0.99
Mean	92.54%	84.05%	92.07%	0.99
Std	1.00%	7.24%	0.58%	0.00

G. RESULTS OF THE CLASSIFICATION OF NORMAL BREATHING, HYPOPNEA EVENTS AND APNEA EVENTS

In this part, 550 samples were selected from the hypopnea, apnea and normal sample sets. The apnea events sample set was formed using a ratio of OA:MA:CA = 6:3:1. Similarly, 10% of the total data set were extracted for Relieff feature screening. Based on the results of feature screening, the remaining 90% of the samples were randomly divided into training, validation and test sets on a ratio of 6:2:2. The results of the test set were used to obtain the final model classification results. The results of feature screening are as follows:

(1) The RMSSD, SDSD, STD and mean of the RR interval of ECG-I and ECG-II;
(2) The VLF of the RR interval of ECG-I;
(3) LFn/HFn of the RR interval of ECG-I and ECG-II;
(4) The mean of the MSE of the second and third layers of the HFCs corresponding to the DWT of the signal in the main CFB of ECG-I and ECG-II energies;
(5) The STD of MSE of the second layer of the HFCs corresponding to the DWT of the signal in the main CFB of ECG-I and ECG-II energies;
(6) The STD of MSE of the third layer of the HFCs corresponding to the DWT of the signal in the main CFB of ECG-II energy;
(7) The Lempel-Ziv complexity of the third and fourth layers of the HFCs corresponding to DWT of the signal in the main CFB of ECG-II energy;

The above 20 features were considered to be the optimal feature set. The detailed classification results are shown in Table 8.

V. DISCUSSION AND CONCLUSION

Many researchers have applied ECG signals to detect SAHS events. ECGs and EMGs have been used for recognition of breathing and movement-related sleep disorders. Bio-signal processing has also been performed by extracting EMG features exploiting entropy and statistical moments; the framework was used to classify participants into four groups: healthy subjects, patients with OSA, patients with restless leg syndrome (RLS) and patients with both OSA and RLS, with a mean accuracy of 72% and a weighted F1-score of 0.57 [7]. Large memory storage and Retrieval (LAMSTAR) ANNs have been combined to predict apnea and hypopnea events, where wavelet transform-based preprocessing was applied to six physiological signals (EEG, HRV, nasal pressure, oronasal temperature, submental EMG, electrooculography) obtained from a set of PSG studies and used to train and test the networks. Apnea prediction achieved a sensitivity and specificity of up to $80.6 \pm 5.6\%$ and $72.8 \pm 6.6\%$, respectively, while hypopnea prediction achieved $74.4 \pm 5.9\%$ and $68.8 \pm 7.0\%$, respectively [8]. A novel methodology based on a single channel ECG for OSA severity classification using a deep learning approach has also been proposed, which focused on the classification between normal subjects (AHI < 5) and severe OSA patients (AHI > 30). An accuracy of 79.45% for OSA severity classification was achieved [9]. Their study conducted feature selection from PSG signals and used a support vector machine to detect SA events. ECG, SaO_2, airflow, abdominal, and thoracic signals were used to provide various frequency, time-domain and non-linear features ($n = 87$). The best results obtained were an accuracy of 95.23%, sensitivity of 94.29% and specificity of 96.17% [10]. A novel approach is proposed to detect sleep apnea events using both the heartbeat interval (HBI) and ECG-derived respiration (EDR) signals. Both HBI and EDR signals were analyzed using reconstructed components or modes using a data-driven signal processing approach, namely sliding mode singular spectrum analysis. The proposed method achieved accuracy values of 94.3%, and 72% for per-recording-based classification of sleep apnea events and normal classes using signals from the apnea-ECG and UCD databases [11]. In [12], features from the HRV, SaO_2, and respiratory effort signals, were extracted from 50 control and 50 OSA patients from the Sleep Heart Health Study database and implemented for minute and subject classifications. In this case, a polynomial kernel showed better performance and the highest accuracy of 82.4% (Sen: 69.9%, Spec: 91.4%) was achieved using a combined-feature classifier.

The above studies show that ECG signals have been successfully applied in the related field of the detection and classification of SAHS events, such as prediction of the severity of OSA patients, recognition of OSA patients with movement-related sleep disorders, classification of SAHS events, detection of sleep apnea events etc. However, most studies were devoted to the detection of SA events. Among them ECG, SaO_2, airflow, abdominal and thoracic signals were used as research objects and a total of 87 frequency, time-domain and non-linear features were extracted. The accuracy, sensitivity and specificity achieved in detecting SA events were almost equal to the results achieved by the method proposed in our study, which utilized only 11 features extracted from the ECG signal itself. Therefore the method proposed by our study not only reduces the cost of collecting signals, but also reduces the amount of calculations involved in the process of extracting features. HBI and EDR signals have also been combined to detect SA events and accuracies of 94.3% and 72% per-recording from the apnea-ECG and UCD databases was achieved, respectively. Besides, when distinguishing between normal breathing, hypopnea events and apnea events, the accuracy rates achieved by their proposed method were 25.06% for apnea events, 51.68% for hypopnea events and 53.66% for normal breathing. However, the method proposed in our research achieved accuracy rates of 90.49% for apnea events, 88.36% for hypopnea events and 92.52% for normal breathing. The HRV, oxygen saturation and respiratory effort signals were combined to predict OSA patients and events, and a highest accuracy of 82.4% has been reported. However, OSA is only one of the most common types of sleep apnea events. The three different types of apnea events were all taken into account in our study and the corresponding samples were reasonably divided according to the different frequency of occurrence. At the same time, our results reached an accuracy of 95.97%, sensitivity of 95.28% and specificity of 96.76% in the detection of SA events. Six physiological signals (HRV, Nasal Pressure, Oronasal Temperature and Submental EMG etc.) and LAMSTAR ANNs were utilized to predict SAHS events. The sensitivity/specificity of apnea and hypopnea events reached 80.6%/72.8% and 74.4%/68.8% respectively. However, in our study, based on only on ECG signals, the accuracy of distinguishing between hypopnea events and the three different types of apnea events all reached values above 90%, and the sensitivity and specificity when classifying hypopnea events and OA events were 92.46% and 90.84% respectively.

The algorithm proposed in this study only used the ECG signal itself to achieve accurate detection of SAHS events. At the same time, it can further distinguish the types of events, that is, identify hypopnea and apnea events. The performance of the algorithm was almost the same in the classification of the three different types of apnea events and hypopnea events, so it is not limited to a specific type of apnea events. The algorithm proposed in this study is efficient, convenient and with low computational cost, and can be applied to wearable devices for home-assisted diagnosis or clinical assessment by doctors in the future. It overcomes the problem of not being able to record PSG data in time to diagnose respiratory disorders. At the same time, the method also solves the problem of excessive signals collected by recording PSG data, which affects sleep comfort at night. Furthermore, it achieves the identification of specific types of SAHS events, thereby facilitating physicians in the determination of the optimal

treatment plans. Therefore, the algorithm proposed in this study has certain clinical application significance.

REFERENCES

[1] P. E. Peppard, T. Young, J. H. Barnet, M. Palta, E. W. Hagen, and K. M. Hla, "Increased prevalence of sleep-disordered breathing in adults," *Amer. J. Epidemiol.*, vol. 177, no. 9, pp. 1006–1014, 2013.
[2] E. W. Terri and F. P. G. Charles, "Cognition and performance in patients with obstructive sleep apnea," in *Principles and Practice of Sleep Medicine*, vol. 1, H. K. Meir, R. Thomas, and C. D. William, Ed., 4th ed. 2005, ch. 85, pp. 1023–1033.
[3] R. B. Berry, R. Budhiraja, D. J. Gottlieb, D. Gozal, C. Iber, V. K. Kapur, C. L. Marcus, R. Mehra, S. Parthasarathy, S. F. Quan, S. Redline, K. P. Strohl, S. L. D. Ward, and M. M. Tangredi, "Rules for scoring respiratory events in sleep: Update of the 2007 AASM manual for the scoring of sleep and associated events," *J. Clin. Sleep Med.*, vol. 8, no. 5, pp. 597–619, Oct. 2012.
[4] V. Vimala, K. Ramar, and M. Ettappan, "An intelligent sleep apnea classification system based on EEG signals," *J. Med. Syst.*, vol. 43, no. 2, p. 36, Feb. 2019.
[5] N. Carroll and M. A. Branthwaite, "Control of nocturnal hypoventilation by nasal intermittent positive pressure ventilation," *Thorax*, vol. 43, no. 5, pp. 349–353, May 1988.
[6] C. Guilleminault, G. Kurland, R. Winkle, and L. E. Miles, "Severe kyphoscoliosis, breathing, and sleep," *Chest*, vol. 79, no. 6, pp. 626–630, Jun. 1981.
[7] D. Jarchi, J. Andreu-Perez, M. Kiani, O. Vysata, J. Kuchynka, A. Prochazka, and S. Sanei, "Recognition of patient groups with sleep related disorders using bio-signal processing and deep learning," *Sensors*, vol. 20, no. 9, p. 2594, May 2020.
[8] J. A. Waxman, D. Graupe, and D. W. Carley, "Automated prediction of apnea and hypopnea, using a LAMSTAR artificial neural network," *Amer. J. Respiratory Crit. Care Med.*, vol. 181, no. 7, pp. 727–733, Apr. 2010.
[9] N. Banluesombatkul, T. Rakthanmanon, and T. Wilaiprasitporn, "Single channel ECG for obstructive sleep apnea severity detection using a deep learning approach," in *Proc. IEEE Region Conf. (TENCON)*, Jeju, South Korea, Oct. 2018, pp. 2011–2016.
[10] X. Li, S. H. Ling, and S. Su, "A hybrid feature selection and extraction methods for sleep apnea detection using bio-signals," *Sensors*, vol. 20, no. 15, p. 4323, Aug. 2020.
[11] H. Singh, R. K. Tripathy, and R. B. Pachori, "Detection of sleep apnea from heart beat interval and ECG derived respiration signals using sliding mode singular spectrum analysis," *Digit. Signal Process.*, vol. 104, Sep. 2020, Art. no. 102796.
[12] H. M. Al-Angari and A. V. Sahakian, "Automated recognition of obstructive sleep apnea syndrome using support vector machine classifier," *IEEE Trans. Inf. Technol. Biomed.*, vol. 16, no. 3, pp. 463–468, May 2012.
[13] J. V. Marcos, R. Hornero, D. Álvarez, F. del Campo, C. Zamarrón, and M. López, "Utility of multilayer perceptron neural network classifiers in the diagnosis of the obstructive sleep apnoea syndrome from nocturnal oximetry," *Comput. Methods Programs Biomed.*, vol. 92, no. 1, pp. 79–89, Oct. 2008.
[14] D. Álvarez, R. Hornero, J. V. Marcos, and F. del Campo, "Feature selection from nocturnal oximetry using genetic algorithms to assist in obstructive sleep apnoea diagnosis," *Med. Eng. Phys.*, vol. 34, no. 8, pp. 1049–1057, Oct. 2012.
[15] A. Bhattacharjee, S. Saha, S. A. Fattah, W.-P. Zhu, and M. O. Ahmad, "Sleep apnea detection based on rician modeling of feature variation in multiband EEG signal," *IEEE J. Biomed. Health Informat.*, vol. 23, no. 3, pp. 1066–1074, May 2019.
[16] M. E. Tagluk and N. Sezgin, "A new approach for estimation of obstructive sleep apnea syndrome," *Expert Syst. Appl.*, vol. 38, no. 5, pp. 5346–5351, May 2011.
[17] M. E. Tagluk, M. Akin, and N. Sezgin, "Classification of sleep apnea by using wavelet transform and artificial neural networks," *Expert Syst. Appl.*, vol. 37, no. 2, pp. 1600–1607, Mar. 2010.
[18] X.-S. Zhang, R. J. Roy, and E. W. Jensen, "EEG complexity as a measure of depth of anesthesia for patients," *IEEE Trans. Biomed. Eng.*, vol. 48, no. 12, pp. 1424–1433, Dec. 2001.
[19] S. M. Pincus and W.-M. Huang, "Approximate entropy: Statistical properties and applications," *Commun. Statist.-Theory Methods*, vol. 21, no. 11, pp. 3061–3077, 1992.
[20] J. S. Richman and J. R. Moorman, "Physiological time-series analysis using approximate entropy and sample entropy," *Amer. J. Physiol.-Heart Circulatory Physiol.*, vol. 278, no. 6, pp. H2039–H2049, Jun. 2000.
[21] S. U. Keyang, J. Zeng, W. Xie, J. Yan, and W. Xie, "Application of EEG approximate entropy in monitoring the depth of anesthesia," *Chin. J. Med. Phys.*, vol. 36, no. 1, pp. 117–120, 2019.
[22] N. Ji, L. Ma, H. Dong, and X. Zhang, "EEG signals feature extraction based on DWT and EMD combined with approximate entropy," *Brain Sci.*, vol. 9, no. 8, p. 201, Aug. 2019.
[23] M. Cukic, D. Pokrajac, M. Stokic, S. Simic, V. Radivojevic, and M. Ljubisavljevic, "EEG machine learning with higuchi fractal dimension and sample entropy as features for successful detection of depression," 2019, *arXiv:1803.05985*. [Online]. Available: https://arxiv.org/abs/1803.05985
[24] X. Zhang and P. Zhou, "Sample entropy analysis of surface EMG for improved muscle activity onset detection against spurious background spikes," *J. Electromyogr. Kinesiol.*, vol. 22, no. 6, pp. 901–907, Dec. 2012.
[25] P. H. Swain and H. Hauska, "The decision tree classifier: Design and potential," *IEEE Trans. Geosci. Electron.*, vol. 15, no. 3, pp. 142–147, Jul. 1977.
[26] L. Breiman and E. S. Robert, "Random forests," *Mach. Learn.*, vol. 45, no. 3, pp. 5–32, 2001.
[27] I. M. Robnik and I. Kononenko, "Theoretical and empirical analysis of ReliefF and RReliefF," *Mach. Learn.*, vol. 53, nos. 1–2, pp. 23–69, 2003.
[28] J. Kim, H. ElMoaqet, D. M. Tilbury, S. K. Ramachandran, and T. Penzel, "Time domain characterization for sleep apnea in oronasal airflow signal: A dynamic threshold classification approach," *Physiol. Meas.*, vol. 40, no. 5, Jun. 2019, Art. no. 054007.
[29] H. ElMoaqet, J. Kim, D. Tilbury, S. K. Ramachandran, M. Ryalat, and C.-H. Chu, "Gaussian mixture models for detecting sleep apnea events using single oronasal airflow record," *Appl. Sci.*, vol. 10, no. 21, p. 7889, Nov. 2020.

YAO WANG was born in 1988. She received the bachelor's degree in engineering from the Department of Biological Sciences and Engineering, South China University of Technology, in 2011, with a focus on biomedical engineering, and the Ph.D. degree in engineering from the Department of Medicine, Tsinghua University, in 2016, with a focus on biomedical engineering. Since 2016, she worked with the Tiangong University, as an Associate Professor. Her main research interests include auditory signal processing and detection, brain–computer interface research based on auditory signals, and auditory and cognitive engineering research.

SIYU JI was born in 1997. She received the bachelor's degree in communication engineering from the Heilongjiang University of Science and Technology, in 2019. She is currently pursuing the master's degree in electronic and communication engineering with Tiangong University. Her current research interests include EEG signal processing and sleep apnea detection.

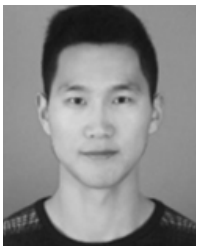

TIANSHUN YANG was born in 1996. He received the bachelor's degree in electronic information and engineering from the Anhui University of Technology, in 2019. He is currently pursuing the degree in information and communication engineering with Tiangong University. His current research interest includes automatic apnea detection.

XIAOHONG WANG was born in 1994. She received the bachelor's degree in communication engineering from the Shijiazhuang University, in 2018. She is currently pursuing the degree with the Tianjin University of Technology. Her current research interest includes automatic apnea detection.

HUIQUAN WANG was born in 1985. He received the bachelor's and Ph.D. degrees in biomedical engineering from the School of Precision Instruments and Optoelectronics Engineering, Tianjin University, the bachelor's degree in international finance from Nankai University, and the Ph.D. degree in instrument science and technology from Tianjin University. From 2011 to 2013, he was a Public Visiting Scholar study with Johns Hopkins University. He is currently the Director of the Department of Biomedical Engineering and the Master Instructor of Tiangong University. His main research interests include wearable medical testing equipment and intervention methods, near-infrared spectroscopy and big data mining algorithms, and multi-modal imaging technology.

XIAOYUN ZHAO was born in 1979. He received the bachelor's and master's degrees from the Medical College, Nankai Univertsity, Tianjin, China, in 2004, and the M.D. degree in respiratory medicine from Tianjin Medical University, Tianjin, in 2016. From 2004 to 2009, he was a Resident Physician with the Tianjin Chest Hospital. Since 2009, he has been an Attending Physician with the Department of Respiratory, Critical Care and Sleep Medicine (PCCSM), Tianjin Chest Hospital, and he has been the Vice Director and the Chief Doctor of RICU and Sleep Center, since 2013. He is currently a Scientist and a Tutor with the Biomedical Engineering Department, Graduate School, Tianjin University, Tianjin; Tiangong University, Tianjin; and Tianjin Medical University, Tianjin. He is the author of more than 40 articles and ten inventions. His research interests include central regulation mechanism of breathing, intermittent swing of pleural pressure during obstruction of airway, and comprehensive complications of sleep breathing disorders. He is a member of the American Thorax Society (ATS), the China Sleep Research Association (CSRA), and several other medical and bioengineering associations.

WANG JINHAI was born in June 1966. He received the Ph.D. degree. He was a Professor, a Postgraduate Tutor, a famous teacher teaching in Tianjin, and a Senior Honorary Researcher with The University of Auckland, New Zealand. He is currently the Leader of the Preparatory Team, School of Life Sciences, Tianjin Polytechnic University; the Leader in biomedical engineering disciplines and majors; the Deputy Director of the Tianjin Medical Diagnosis and Treatment Technology Engineering Center, Tianjin; the Electronic Information and Engineering Practice Teaching Team Leader, Tianjin Polytechnic University; and the Signal Leader of the Scientific Research and Innovation Team (New technologies for detection and medical electronic diagnosis and treatment). His part-time social jobs include the Vice President of the Tianjin Intelligent Science and Technology Research Association, the Executive Director of the Tianjin Biomedical Engineering Society, the Director of the Tianjin Robotics Society, the Director of the Tianjin Microcontroller Society, the Director of the Tianjin Institute of Communication Higher Education Working Committee, the Senior Member of the China Institute of Electronics, a member and an expert of the Tianjin Organizing Committee of the National College Student Electronic Design Competition, and an expert of the Tianjin Science and Technology Support Project Evaluation.